

Ground-penetration radar detection of Root-mass in a Tree Groove in Southwestern Nigeria.

*Muslim Babatunde Aminu, Femi Ologunaye

Adekunle Ajasin University
Akungba-Akoko,
Nigeria

Email: muslimaminu@gmail.com

Abstract

*In this study, we present the results of a ground-penetrating radar (GPR) survey aimed at imaging the lateral root systems of a section of a tree groove lined by the *Tectona Grandis* (Teak) species. This was to set the basis for deploying a multi-frequency GPR system for the non-invasive monitoring of root-mass development and evaluation of plant development and health. The survey involved a single GPR Transect with a total length of 60.1 m established along the middle of a line of matured Teak trees. Data was collected at 250 MHz, 500 MHz and 1000 MHz, simultaneously using a wheel-triggered Utsi Trivue system. Data processing involved a dewow, static corrections, gain application and background removal. A root zone consisting of two layers was delineated and a total of 159 hyperbolae were interpreted as roots. The roots were limited to the shallow subsurface, the upper 1.1 m of a potential root zone 1.6 m deep. Imaged roots generally occur in clusters that create much disturbance of the otherwise continuous reflections in the root zone. Often, roots may be laterally offset from the location of tree bases on the Transect. We further identified a potential set of laterally migrating roots in a zone of undisturbed ground outside the main groove indicating the lateral reach of the usually shallow roots of the Teak tree. The results set the basis for further work in root-mass estimation and monitoring tree health within our team.*

Keywords: ground-penetrating radar, root zone, root clusters, laterally migrating roots, tree health.

INTRODUCTION

Ground-penetrating radar (GPR) is a useful non-invasive geophysical tool for the detection and characterization of both naturally occurring and man-made features buried within the shallow subsurface (0.25 to 2 m depth) (Butnor *et al.*, 2001; Utsi 2017). Due to its easy-to-deploy and rapid implementation nature, it has been used widely in civil engineering (Maierhofer, 2003; Salucci *et al.*, 2014), geophysical investigations (Jol *et al.*, 1996; Carrière *et al.*, 2013), archaeological research (Conyers, 2013), quantification of soil water content (Klotzsche *et al.*, 2018), in mapping buried utilities (Ni *et al.*, 2010; Porsani *et al.*, 2012), and more.

The GPR technique involves sending electromagnetic (EM) waves (50–2600 MHz) into the shallow subsurface and measurement of the amplitudes and times of the energy reflected from electrically contrasting interfaces (Wielopolski *et al.*, 2000; Daniels, 2004). Reflections arise due to differences in the dielectric properties of adjacent materials and the soil (Bain *et al.*, 2017; Utsi 2017). In addition to object location, the GPR technique allows the estimation of the size and orientation of the object, as well as moisture content (Ferrara *et al.*, 2013).

*Author for Correspondence

A recent and exotic application of the GPR technique is in the non-invasive phenotyping of root-mass development in forests and agricultural fields (Liu *et al.*, 2018; Lombardi, *et al.*, 2021). Due to the contrast in dielectric properties generated at the soil-root-mass interface, the GPR technique has shown significant promise in the detection and mapping of living root systems when soil moisture and salinity conditions permit (Butnor *et al.*, 2001. Teare *et al.*, 2021).

Plant root development plays a critical role in agricultural productivity. It determines the rate of uptake of critical resources (water, nutrients, agrochemicals), provides rigid support against environmental elements (wind, erosion and animals), enables the storage of essential resources (water, carbohydrates, nutrients), mediates interactions with pathogenic and beneficial organisms in the rhizosphere, and controls biogeochemical cycling and recycling in terrestrial ecosystems (Liu *et al.*, 2018).

Nichols *et al.* (2017), used GPR to evaluate the effectiveness of three different prototype permeable pavement designs in reducing pavement damage caused by street tree roots. The study involved initial tests in a simulated test environment that was later replicated in the field. Positive root identifications were recorded for all three prototype pavements but the accuracy of the GPR results was found to vary according to soil type, depth of aggregate sub-base, amount of water contained within the soil, and the buried objects used for calibration. The three-dimensional nature (overlapping) of genuine tree roots also affected the detection accuracy of the GPR in the field.

Zhu *et al.* (2014), used an advanced 3D Ground Penetrating Radar (3D GPR) consisting of 500 MHz and 800 MHz bow-tie antennas, to detect coarse tree roots and to estimate root biomass in the field. The study obtained full-resolution 3D imaging results of tree root systems. A continuity-of-pixel intensity searching algorithm was proposed and used to detect and delineate two coarse roots (>5 cm). The study proposed two indices for root mass phenotyping, a linear regression index to estimate total root biomass which achieved an error <10% and a magnitude width index to estimate root diameter with a 13-16% error.

Bain *et al.* (2017), conducted an experimental evaluation of key factors affecting root biomass estimation including multiple scanning directions, root crossover, and root versus soil moisture content, using a 1500 MHz GPR system. By combining four scanning directions, a significant relationship between GPR signal reflectance and coarse root biomass was achieved. When moisture content was allowed to equalize with the surrounding soil, GPR failed to detect dead root mass. However, the 1500 MHz antenna allowed the identification of roots in close proximity to each other, as well as roots, shadowed beneath shallower roots.

Liu *et al.* (2018), assessed the feasibility of utilizing GPR to detect fine roots in field trials at four locations with different soil types and soil moisture conditions. Varieties of winter wheat and energy cane were scanned with a 1600 MHz GPR antenna and soil cores were collected immediately after scanning in order to measure root parameters. Pixelated image analysis was used to assess the relationships between the GPR signal and root parameters. The study found significant correlations between GPR indices and root parameters depending on soil conditions. Wet clay soils provided greater accuracy in root estimation compared to dry sandy soils and estimated root parameters from GPR showed lower variation than measured roots.

Teare *et al.* (2021), utilized GPR for effective estimation of bulked root mass as a proxy for cassava root mass under varying soil conditions. The goal was to establish good practice in GPR estimation of root mass and to investigate the effect of soil water content on measurement

and detection. Significant correlation between GPR data and daikon root mass was obtained for three of the five irrigation treatments with correlation strength improving with increased soil water content and decreased variability in soil water content between plots. The results were the first to show that wet soils can improve the predictive quality of GPR data in root-mass detection and estimation.

In this study, we present the results of a GPR survey along a Transect in a local tree groove suspected to be established over a section containing subsurface clayey layer in southwestern Nigeria.

MATERIALS AND METHOD

Study Site: This study was carried out on Adekunle Ajasin University Campus located in Akungba-Akoko in the northeastern region of Ondo State, southwestern Nigeria (Figure 1). Akungba-Akoko is located between $05^{\circ} 43' E$ and $05^{\circ} 47' E$, and $07^{\circ} 27' N$ and $07^{\circ} 31' N$. The township bounds consist of a gently sloping central low-lying region surrounded in a perimeter-like pattern by high-rising granitic hills to the north, west, east and southeast. Topographic relief is generally greater than 345 m above sea level with surrounding hills rising to 420 m above sea level. The rocks of the area consist of the migmatite-gneiss complex of the basement rocks of south-western Nigeria (Rahaman, 1989); a suite made up of biotite-rich grey gneiss, granite gneiss and lesser amounts of charnockites (Ogunyele *et al.*, 2019). Drainage is provided by seasonal streams which initiate from high reliefs in the northeast. Regolith development is thin, hardly exceeding a few meters. The study area is a tree groove in the Western Campus of Adekunle Ajasin University Akungba-Akoko between the Faculty of Science building and a quadrangle of 4 nos. 300 capacity lecture halls known as the ETF Quadrangle as shown in Fig. 1.

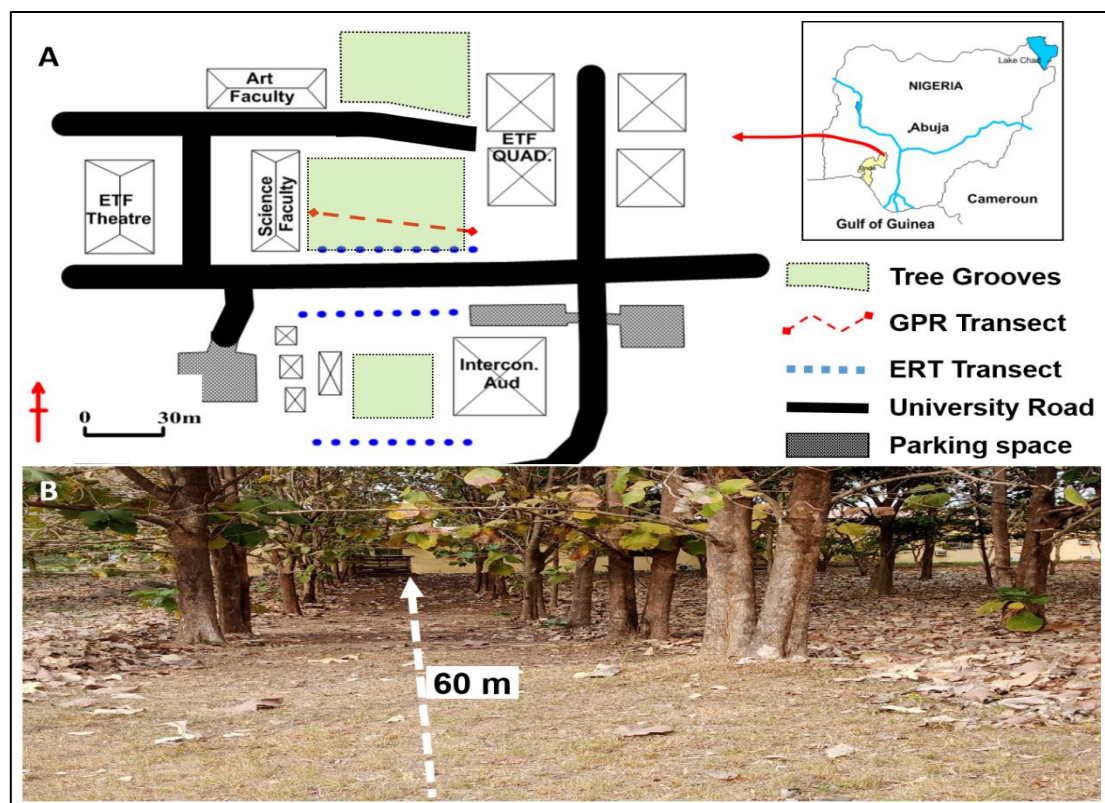


Fig. 1. (A) Schematic of the study site. GPR Transect, in red dashed line, runs roughly east-west (Modified after Aminu 2015); (B) Tree groove with GPR Transect in white dashed line. The arrowhead indicates the survey direction.

GPR Principle: The propagation of radar signals through a medium is governed by the physical principles related to EM waves (Evans *et al.*, 2006). In the GPR Technique, high-frequency electromagnetic pulses (radar) from a transmitting antenna (or an array of antennas) are sent into the subsurface and record is made of the time taken for reflected energy to return to a receiver antenna (Rhee *et al.*, 2021). The passage of radar waves through the medium is dependent on a number of factors including the type of the material of the medium and its condition, and the nature and amount of water it contains. These properties determine the dielectric constant of the medium. The dielectric constant controls the speed of the radar pulse through the medium and the partitioning of its energy between reflection back to the surface and transmission to deeper layers (Rhee *et al.*, 2021). If two materials have sufficiently contrasting dielectric properties, some radar energy is reflected to the surface from the material boundary (Figure. 2).

GPR systems operate over a wide range of frequencies, usually, 100 MHz to 2000 MHz (Evans *et al.*, 2006), with higher frequencies (≥ 400 MHz) providing higher resolution in the shallow sections of the material but due to the preferential attenuation of high frequencies, they offer a much-limited depth of investigation (Rhee *et al.*, 2021). This encourages their use for detailed near-surface surveys such as pavement monitoring and mapping reinforced concrete rebar conditions, and root-mass developments. Lower frequencies (≤ 400 MHz) generally provide greater depths of investigation but lower resolution capacity. They therefore find much use in geological mapping (Zajc *et al.*, 2014), deep foundation studies (Abdullah *et al.*, 2022), and deep archaeological studies (Zhao *et al.*, 2018).

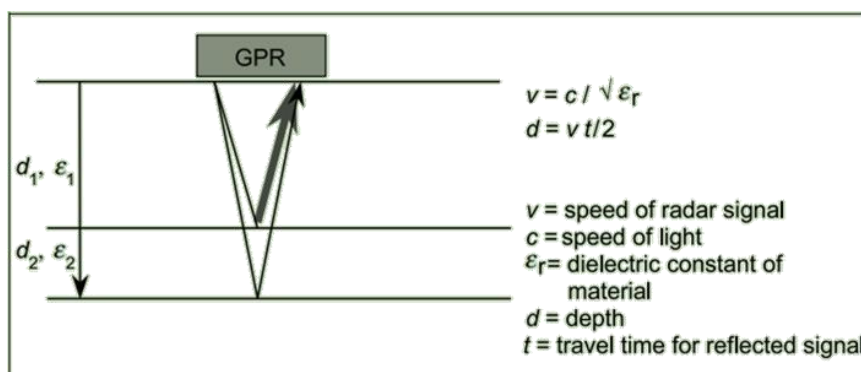


Fig 2. Schematic of GPR Technique with parameters for the calculation of radar pulse speed and depth (Evan *et al.*, 2006)

Survey setup and procedure: A GPR Transect was surveyed in this study. The GPR Transect is 60.1 m long and was surveyed from the proximate southeastern end of the groove to the southwestern end (Figure 1). The transect travels in between two roughly east-west lines of trees. Trees on either side of the transect are of the *Tectona Grandis* (common name: Teak) species known to have superficial branching lateral roots often no deeper than 50 cm. Teak roots generally show complex reticulate branching and intertwining and may extend laterally up to 15m. Trees in this groove are over 10 years old and reach heights above 20 m. GPR data was collected using a triple-frequency Utsi Electronic Trivue system with bandwidths of 125 - 500 MHz, 200 - 800 MHz and 500 - 2000 MHz centered on 250 MHz, 500 MHz and 1000 MHz, respectively. The antennas are co-centred. Record times were 80 ns, 60 ns and 40 ns for the 250 MHz, 500 MHz and 1000 MHz records, respectively. Triggering was via an encoder wheel system which also records the length of the transects. Data were collected in October towards the end of the rainy season. Notations were made of the lateral locations of trees (Table 1). Data processing was accomplished in Reflex-Win Version 10.1 and followed a sequence

including (Table 2): (1) Dewow, (2) Static correction, (3) Gain, and (4) Background removal. The outputs were 2D GPR radar-grams plotted in time (ns) versus lateral position. The final sections are presented in grayscale as this provides the best opportunity to identify features. After data analyses, three trenches were made to calibrate interpreted root depths and the propagation velocity in the area.

Table 1: Lateral position of trees noted along the GPR Transect.

SNo.	Feature	Position (m)
1	Transect starts	0,
2	Tree 1	7, 14, 19.5, 24, 32, 37, 44, 50, 54, 60
3	Transect ends	60.1

Table 2: Processing Sequence applied to the GPR data.

SNo.	Processing Sequence ID	Parameter		
		250 MHz	500 MHz	1000 MHz
1	Dewow	64 ns	32 ns	16 ns
2	Static correction	Variable	Variable	Variable
3	Gain (exponential)	0.5	1	2
4	Background removal	Automatic	Automatic	Automatic

RESULTS AND DISCUSSION

The presentation in this study involves only the 500 and 1000 MHz GPR (Figure 3). These frequencies sufficiently imaged the root zone at the study area and enabled ample interpretation of roots. The 250 MHz section provided little to no information on the object of the investigation (roots). The 1000 MHz section provided a very high resolution of root systems in the very shallow subsurface (< 0.4 m). It further allowed the resolution of many individual roots including roots whose reflection hyperbolae overlap in the 500 MHz section and those that occur vertically below shallower roots. Conversely, the 500 MHz section allowed the identification of deeper roots and allowed the imaging of the overall morphology and depth of the root zone at the study site. The Hilbert envelope attribute helped to map the individual layers of the root zone at the site.

The 'root zone' generally is less than 1 m. The exception is in the 12 - 35 m region where its soil depth may reach up to 1.6 m forming a convex downwards basin-like morphology (Figure 3c & 3d). This morphology could be partly related to the nature of the shallow sections of the clayey aquitard known to occur along the Transect. Details can be found in Aminu, 2015. The 'root zone' appears to consist of two distinct layers. The upper layer consists of high amplitude fairly continuous radar responses in the top 0.4 m of the 500 MHz section (Dig to get interpretation). This layer appears to reach a maximum of 0.46 m in the two extremes of the Transect. The lower layer consists of low amplitude radar responses with thickness varying from 0.3 m at the two ends of the Transect to 1.2 m in the basin-like region. The radar responses in this layer are less continuous, laterally, and frequently are interrupted by the presence of reflection hyperbolae. Aminu 2015, imaged an overburden characterized by a very low apparent resistivity response (<200 Ωm) with a thickness generally in excess of 6 m thickness at the site. The basin-like morphology of the second layer is approximately coincident with the imaged aquitard of Aminu, 2015. The base of the overburden imaged in Aminu 2015 has not been delineated in the current survey. It likely reflects the top of basement rocks in the area.

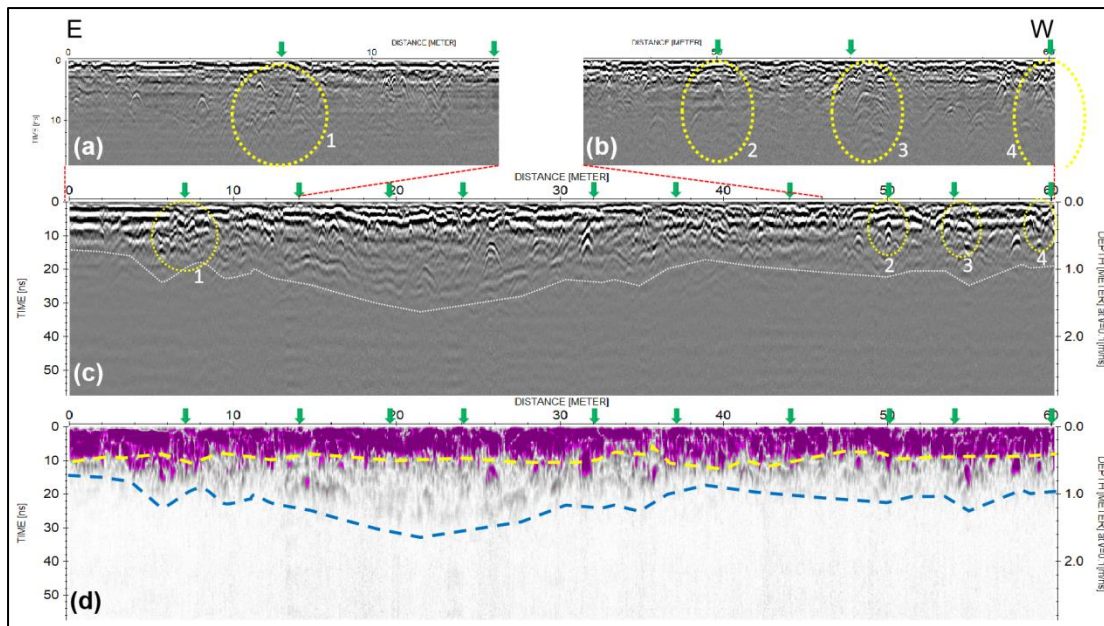


Fig. 3. Composite panel of GPR imaging along the Transect: (a) and (b) are enlarged 1000 MHz sections, (c) 500 MHz response, (d) Hilbert Envelope response of the 500 MHz data (Purple indicates high amplitude). Green arrows indicate the location of Tree bases (*Tectona Grandis*).

A total of 144 hyperbolae were identified and interpreted from the 500 MHz section. A further 15 hyperbolae not apparent on the 1000 MHz were identified on the 500 MHz to make a total of 159. Roots are roughly cylindrical in cross-section and show as hyperbolae in radar section (Utsi 2017). The 15 hyperbolae identified from the 1000 MHz possibly represent roots with a diameter lower than the minimum resolution of the 500 MHz antenna (Utsi 2017). On the Hilbert envelope section (Figure 3d) hyperbolae in the upper layer of the root zone cannot be discriminated from each other. In the lower layer, major hyperbolae appear as concave downward cusps. The tree groove is known to be largely free of buried utilities and we consider all identified hyperbolae as potential roots of the *Tectona Grandis*. The depth range for interpreted roots was from the surface to a maximum of 1.09 m (using a velocity of 0.1 m/ns). Results from two trenches in the groove confirmed the presence of multiple roots of varying thicknesses and depths of burial. Burial depths were generally within the range of depths estimated from the GPR section ($\pm 7\%$). These compare well with error ranges reported by (Butnor *et al.*, 2001; Nichols *et al.*, 2017). We note that hyperbolae occur in clusters with considerable overlap between adjacent hyperbolae. Frequently, hyperbolae occur vertically stacked one above the other. This clustering and vertical stacking is likely related to the branching and intertwining of roots common with the *Tectona Grandis*. The clustering and vertical stacking of roots make individual roots indistinguishable and complicate root-mass estimation from GPR data (Bain *et al.*, 2017). Hyperbolae clusters occur proximate to the surface locations of Tree bases in the groove (Figure 3a & 3b). They may however be displaced by up to 1.0 m from the observed surface location of the trees (Figure 3b). From visual inspection at the site, surface roots of the *Tectona Grandis* radiate in all directions and away from the tree bases they may cross the GPR Transect at a considerable offset. We consider that the shallow depths of hyperbolae along the Transect (generally not more than 1.1 m), their tendency to cluster together and occur vertically stacked one over another, and the sometimes significant lateral offsets from tree bases all lend credible evidence that the interpreted hyperbolae are related to lateral roots of the *Tectona Grandis* within the groove. These results are comparable to several previous studies which have successfully detected tree roots at specific sites (Nichols *et al.*, 2017; Liu *et al.*, 2018).

In the 0 - 6 m region of the Transect, two strong amplitude highly continuous reflections occur on the 500 MHz section at 0.2 and 0.5 ns, respectively. This region falls outside the location of trees in the groove and appears to indicate little to no root presence in the region with the exception of a disruption of the deeper reflection at 2 - 3 m. However, the 1000 MHz section indicates the occurrence of multiple hyperbolae in the 2 - 5 m region. This can imply the presence of multiple root systems in the area (Figure 3a). As this region is outside the Tree area, the hyperbolae likely represent the presence of laterally migrating roots from trees on the periphery of the groove. Roots of the *Tectona Grandis* are known to laterally migrate up to 15 m (Orwa *et al.*, 2009). This region therefore is within reach of roots of trees located on the edge of the groove, and likely represents an area of little overburden disturbance devoid of the presence of large root systems and complexly intertwined root systems.

CONCLUSION

We have utilized a multi-frequency GPR system to image tree roots in a groove on Adekunle Ajasin Campus. The goal was to evaluate the root-mass detection capacity of the GPR system with a view to adapting it for non-invasive and rapid monitoring of root development and tree/plant health in the region. The root zone is shallow generally less than 1.6 m. The imaged root systems within the groove do not extend beyond 1.1 m depth and in character correlate well with the shallow nature of the lateral roots of the *Tectona Grandis*, the tree species along the Transect. The hyperbolae signatures of the roots tend to cluster in groups and overlap and occur with multiple roots implied to stack vertically above one another in agreement with the intertwining nature of the roots of the *Tectona Grandis*. The study indicates that multi-frequency GPR surveys provide a greater opportunity to detect and image tree roots. We have not attempted to estimate the size of the root mass of the trees in this study. To do so, it will be necessary to estimate the thicknesses of the imaged roots. This we hope to do subsequently.

Acknowledgments

We are grateful to the Agrosoil Research Team at Adekunle Ajasin University for providing access to the Trivue GPR System and the Reflexw-10 software used in this study.

References

- Abdullah, M. S., Karim, H. H. & Samueel Z. W. (2022). Investigation structural settlement by Ground Penetrating Radar (Case study) IOP Conference. Series: *Earth and Environmental Science*, 961 (2022) 012037 IOP Publishing, DOI:10.1088/1755-1315/961/1/012037
- Aminu, M. B. (2015). Electrical Resistivity Imaging of a Thin Clayey Aquitard Developed on Basement Rocks in Parts of Adekunle Ajasin University Campus, Akungba-Akoko, South-western Nigeria. *Environmental Research, Engineering and Management*, 71(1), 47-55.
- Bain, J. C.; Day, F. P. & Butnor, J. R. 2017. Experimental Evaluation of Several Key Factors Affecting Root Biomass Estimation by 1500 MHz Ground-Penetrating Radar. *Biological Sciences Faculty Publications*, 226. https://digitalcommons.odu.edu/biology_fac_pubs/226
- Butnor, J. R., Doolittle, J., Kress, L., Cohen, S. & Johnsen K. H. 2001. Use of ground-penetrating radar to study tree roots in the southeastern United States. *Tree Physiology*, 21, 1269–1278. <https://doi.org/10.1093/treephys/21.17.1269>
- Carrière S. D., Chalikakis K., Sénéchal G., Danquigny C., & Emblanch C., 2013. Combining electrical resistivity tomography and ground penetrating radar to study geological structuring of karst unsaturated zone. *Journal of Applied Geophysics*, 94, 31-41.
- Conyers L. B., 2013. *Ground-penetrating radar for archaeology*. Rowman and Littlefield Publishers, Alta Mira Press, Latham, MD, USA.

- Daniels, D. J. 2004. *Ground Penetrating Radar*, 2nd ed.; Institution of Electrical Engineers: London, UK. <http://dx.doi.org/10.1049/pbra015e>
- Evans, R., Frost, M., Stonecliffe-Jones, M. & Dixon, N. 2006. Ground-penetrating radar investigations for urban roads. *Proceedings of the Institution of Civil Engineers Municipal Engineer*, 159 (2), 105-111. <https://doi.org/10.1680/muen.2006.159.2.105>
- Ferrara, C., Barone, P. M., Steelman, C., Pettinelli, E., & Endres, A. L. 2013. Monitoring shallow soil water content under natural field conditions using the early-time GPR signal technique. *Vadose Zone Journal*, 12 (4): 1–9. doi:10.2136/vzj2012.0202.
- Jol H. M., Smith D. G., & Meyers R. A., 1996. Digital ground penetrating radar (GPR): A new geophysical tool for coastal barrier research (examples from the Atlantic, Gulf and Pacific coasts, USA). *Journal of Coastal Research*, 12 (4), 960-968. <http://www.jstor.org/stable/4298546>.
- Klotzsche, A., Jonard, F., Looms, M. C., van der Kruk, J., & Huisman, J. A. (2018) Measuring soil water content with ground penetrating radar: a decade of progress. *Vadose Zone Journal*, 17:180052. <https://doi.org/10.2136/vzj2018.03.0052>
- Liu, X., Dong, X., Xue, Q., Leskovar, D. I., Jifon, J., et al. 2018. Ground penetrating radar (GPR) detects fine roots of agricultural crops in the field. *Plant Soil*, 423, 517–531. <https://doi.org/10.1007/s11104-017-3531-3>
- Lombardi, E., Ferrio, J. P., Rodríguez-Robles, U., de Dios, V. R. & Voltas, J. 2021. Ground-Penetrating Radar as phenotyping tool for characterizing intraspecific variability in root traits of a widespread conifer. *Plant Soil*, 468, 319–336. <https://doi.org/10.1007/s11104-021-05135-0>
- Maierhofer C., 2003. Nondestructive evaluation of concrete infrastructure with ground penetrating radar. *Journal of Materials and Civil Engineering*, 15, 287-297. [https://doi.org/10.1061/\(ASCE\)0899-1561\(2003\)15:3\(287\)](https://doi.org/10.1061/(ASCE)0899-1561(2003)15:3(287))
- Ni, S. H., Huang, Y. H., Lo, K. F. & Lin, D. C. 2010. Buried pipe detection by ground penetrating radar using the discrete wavelet transform. *Computers and Geotechnics*, 37, 440–448. <https://doi.org/10.1016/j.compgeo.2010.01.003>
- Nichols, P., Adrian, M. & Terry, L. 2017. Using Ground Penetrating Radar to Locate and Categorise Tree Roots Under Urban Pavements. *Urban Forestry and Urban Greening*. <http://dx.doi.org/10.1016/j.ufug.2017.06.019>
- Ogunyele, A. C., Oluwajana, O. A., Ehinola, I. Q., Ameh, B. E. & Salaudeen, T. A. 2019. Petrochemistry and petrogenesis of the Precambrian Basement Complex Rocks around Akungba-Akoko, southwestern Nigeria. *Material and Geoenvironments*, 66(3) 173-183. <https://doi.org/10.2478/rmzmag-2019-0036>
- Orwa, C., Mutua, A., Kindt R., Jamnadass, R. & Anthony. S. 2009. *Agroforestry Database: A tree reference and selection guide version 4.0* (<http://www.worldagroforestry.org/sites/treedbs/treedatabases.asp>)
- Porsani, J. L., Ruy, Y. B., Ramos, F. P. & Yamanouth, G. R. B. 2012. GPR applied to mapping utilities along the route of the Line 4 (yellow) subway tunnel construction in São Paulo City, Brazil. *Journal of Applied Geophysics*, 80, 25–31. <https://doi.org/10.1016/j.jappgeo.2012.01.001>
- Rahaman, M. A. (1989). Review of the Basement Geology of South-Western Nigeria. In: Kogbe, C. A. (eds). *Geology of Nigeria* (2nd ed.) Rockview Nige Limited, Jos, (pp. 39-56).
- Rhee, J.-Y., Park, K.-T., Cho, J.-W. & Lee, S.-Y. 2021. A Study of the Application and the Limitations of GPR Investigation on Underground Survey of the Korean Expressways. *Remote Sensing*, 13, 1805. <https://doi.org/10.3390/rs13091805>
- Salucci M., Tenuti L., Nardin C., Oliveri G., Viani F., Rocca P. & Massa A., 2014. Civil Engineering Applications of Ground Penetrating Radar Recent Advances@ the ELEDIA Research Center. *EGU General Assembly Conference Abstracts*, 16, 1945.

- Teare, B. L., Ruiz, H., Agbona, A., Wolfe, M., Dobрева, I., Adams, T. & Selvaraj, M. 2021. Effect of Soil Water on GPR Estimation of Bulked Roots, Methods, and Suggestions. *Research Square*. <https://doi.org/10.21203/rs.3.rs-907807/v1>
- Utsi, E. C. 2017. *Ground Penetrating: Radar Theory and Practice*. Butterworth-Heinemann. P. 205. <https://doi.org/10.1016/B978-0-08-102216-0.00016-3>.
- Wielopolski, L., Hendey, G. & McGuigan, M. 2002. Imaging tree root systems in situ. *Proceeding of SPIE*, 4080. *Ninth International Conference on Ground Penetrating Radar*, (12 April 2002), <https://doi.org/10.1117/12.462319>
- Zajc, M., Pogačnik, Ž. & Gosar, A. 2014. Ground penetrating radar and structural geological mapping investigation of karst and tectonic features in flyschoid rocks as geological hazard for exploitation, *International Journal of Rock Mechanics and Mining Sciences*, 67, 78-87, <https://doi.org/10.1016/j.ijrmms.2014.01.011>.
- Zhao, W., Forte, E., Fontana, F., Pipan, M. & Tian, G. 2018. GPR imaging and characterization of ancient Roman ruins in the Aquileia Archaeological Park, NE Italy, *Measurement*, 113, 161-171, <https://doi.org/10.1016/j.measurement.2017.09.004>.
- Zhu, S., Huang, C., Su, Y. & Sato, M. 2014. 3D Ground Penetrating Radar to Detect Tree Roots and Estimate Root Biomass in the Field, *Remote Sensing*, 6, 5754-5773, doi:10.3390/rs6065754 ISSN 2072-4292